

**Aleksandrs Nevskis**

**DYNAMIC PROPERTIES OF THE AIRCRAFT'S  
FULL-SCALE COMPONENT TEST SETUP AND ITS  
VIBRATION-BASED SYSTEM OF STRUCTURAL  
HEALTH ASSESSMENT**

Summary of the Doctoral Thesis



**RIGA TECHNICAL UNIVERSITY**

Faculty of Mechanical Engineering, Transport and Aeronautics  
Institute of Aeronautics

**Aleksandrs Nevskis**

Doctoral Student of the Study Programme “Transport”

**DYNAMIC PROPERTIES OF THE AIRCRAFT'S  
FULL-SCALE COMPONENT TEST SETUP AND  
ITS VIBRATION-BASED SYSTEM OF  
STRUCTURAL HEALTH ASSESSMENT**

**Summary of the Doctoral Thesis**

Scientific supervisor  
Professor Dr. habil. sc. ing.  
VITĀLIJS PAVELKO

Scientific consultant  
Professor Dr. habil. sc. ing.  
MĀRTIŅŠ KLEINHOFS

RTU Press  
Riga 2023

Ņevskis, A. Dynamic Properties of the Aircraft's Full-scale Component Test Setup and its Vibration-based System of Structural Health Assessment. Summary of the Doctoral Thesis. Riga: RTU Press, 2023. 31 p.

Published in accordance with the decision of the Promotion Council "RTU P-22" of May 20, 2022, Minutes No. 04030-9.16.1/4.

<https://doi.org/10.7250/9789934229374>

ISBN 978-9934-22-937-4 (pdf)

# **DOCTORAL THESIS PROPOSED TO RIGA TECHNICAL UNIVERSITY FOR THE PROMOTION TO THE SCIENTIFIC DEGREE OF DOCTOR OF SCIENCE**

To be granted the scientific degree of Doctor of Science (Ph. D.), the present Doctoral Thesis has been submitted for the defence at the open meeting of RTU Promotion Council on 30 June, 2023 at 13:00 at the Faculty of Mechanical Engineering, Transport and Aeronautics of Riga Technical University, 6B Ķīpsālas Street, Auditorium 513.

## **OFFICIAL REVIEWERS**

Dr. sc. ing. SANDRIS RUČEVSKIS

Riga Technical University

Dr. sc. ing. HELGE PFEIFER

Katholieke Universiteit Leuven, Belgium

Dr. habil. sc. ing. SERGEJ IGNATOVICH

National Aviation University, Ukraine

## **DECLARATION OF ACADEMIC INTEGRITY**

I hereby declare that the Doctoral Thesis submitted for the review to Riga Technical University for the promotion to the scientific degree of Doctor of Science (Ph. D.) is my own. I confirm that this Doctoral Thesis had not been submitted to any other university for the promotion to a scientific degree.

Aleksandr NEVSKY



March 15, 2023

The Doctoral Thesis has been written in English. It consists of an introduction, 9 chapters, conclusions, 74 figures, 7 tables; the total number of pages is 90. The Bibliography contains 68 titles.

## Contents

1. Introduction. The aim and main problems of research .....	5
2. Overview of the problem of aerospace structure test.....	6
3. Analytical study and computer-aided simulation of dynamic properties of aircraft component in full-scale test.....	7
3.1. On the Properties of Solutions of the Structural Dynamics of Elastic Systems.....	7
3.2. Simple Example: A Cantilever Beam With an Elastic Clamping.....	7
3.3. Dynamic Properties and Response of the Structure.....	8
4. Vibration-based detection of structural damage in full-scale test.....	10
4.1. Fundamentals of method (dynamic properties, dynamic response to different types of excitation, EMA and OMA approaches of dynamic properties evaluation and damage detection, board band excitation and frequency response function, transience function).....	10
4.2. General problems of vibration-based method (VBM) application .....	10
4.3. The basic idea of innovative approach of a damage detection by VBM: the use of group evolution of higher modes.....	11
5. Experimental study and method validation .....	13
5.1. Full-scale comp used in the test.....	13
5.2. The objective of test and equipment .....	17
5.3. Test results .....	19
5.4. Discussion and feature extraction .....	20
6. Statistical Estimation of Perspective Damage Index for Vibration-Based Structural Health Monitoring..	22
6.1. About Test Setup and Measurement Equipment.....	22
6.2. Some Important Results of Research.....	22
6.3. Data Acquisition and Statistical Analysis.....	23
7. Final discussion of integral damage index and conclusions .....	27
References:.....	29

## **1. Introduction. The aim and main research problems**

**Relevance.** To ensure the reliability of the operation of aviation equipment, the regulatory documents provide for a large range of activities, the purpose of which is to prove that the design meets the requirements. A key link in ensuring reliability is the testing of full-size structures or individual, most critical components thereof. The procedure for such tests is extremely expensive and, as a rule, takes considerable time. Therefore, improving the methods of planning, organizing and conducting tests, collecting and processing information, solving problems of control and test automation represent a range of topical scientific and technical problems, on the basis of which the effectiveness of the tests and the reliability of their results depend. Some of these problems determine the motivation of this study.

### **The aim of Doctoral Thesis**

Investigation of the dynamic properties of test complex of aircraft full-scale structural component and an analysis of a version of the vibration-based system of structural health monitoring (SHM).

### **The main research problems**

1. Investigation of some general effects of the boundary conditions and their adequate description at the structural dynamic analysis.
2. Consideration of a simplified model of the elastically supported beam to evaluate the effects of the support compliance to the basic dynamic characteristics.
3. More complex modeling of the body elastic attachment.
4. General problem of vibration-based method (VBM) of nondestructive testing (NDT) application for SHM in the full-scale test of aircraft components
5. Development of a solution for a relatively small structural damage detection using operational excitation (in the frame of the operational modal analysis (OMA) approach).
6. Development of perspective appropriate damage index for detection of small structural damage in the large structural component.
7. Estimation of accuracy and reliability of the developed VBM.

### **Scientific novelty and areas of application**

1. Investigation of some general properties of the boundary conditions and their adequate description in the structural dynamic analysis.
2. A simplified model of the elastically supported beam chosen for evaluation of the effect of elastic constrains for the basic dynamic characteristics.
3. A more complex general model of the body elastic attachment has been modelled.
4. Application of vibration-based method of NDT for SHM in the full-scale test of aircraft components.
5. Innovative analytical solution for a relatively small structural damage detection using operational excitation (in the frame of the OMA approach).
6. Perspective damage index for detection of small structural damage in the large structural component using correlation of a structure dynamic frequency response.

7. Statistical estimation of accuracy and reliability of developed VBM and evaluation of probability of the structural damage detection.
8. The results of the Doctoral Thesis are oriented towards practical use in dynamic trials of aviation techniques.
9. The variant developed by the vibration-based design condition monitoring system can be useful both for monitoring aviation designs and other industry structures and for their operation.

## **2. Overview of the problem of aerospace structure test**

The review chapter provides an analysis of the current state of the problem of testing aviation and space technology using the Internet, literature sources and own experience in planning, organizing and conducting full-scale tests. The main focus was on the following issues:

- Aircraft structure test and classification.
- Full-scale test aircraft component for strength evaluation.
- Equipment of full-scale test, control and measurement.
- Structural damages, their description, and severity.
- Structural damage detection technologies, equipment, and signatures.
- Motivation of Thesis, principal purpose, and tasks.

Regardless of the final applied goal, the damage identification in full-scale components of complex mechanical systems implies a complete or partial determination of their dynamic properties. Frequently, such an adequate solution cannot be obtained by using theoretical analysis only. In these cases, an accurate test provides the necessary information to solve the problem of dynamic identification [1]. There is a number of research works and developments in mechanical, civil and aerospace engineering dedicated to the vibration analysis for different applications. A corresponding overview of this information can be found in [2]–[8].

Usually two types of tests are used in practice: forced and ambient vibration tests. The first of them is coupled with the technique of empirical modal analysis (EMA) which is presented in [9]. The EMA technique is more complete and accurate. It helps to identify the dynamic properties of a system but requires special equipment to excite vibrations. Despite this, the EMA technique has been used in the determination of the dynamic characteristics of even very large structures [10]–[13]. Another method – operational modal analysis (OMA) uses output only. It is cheaper and faster than EMA and can be easily applied to large structures [14].

The computational simulation can be useful for both the test arrangement and interpretation of their results. The computational simulation can improve the effectiveness of the analysis and solve the key problems of structural health monitoring and dynamic system identification [15]–[18], coupling technique [19], [20], structural integrity [21], [22], nonlinear dynamics [23], especially, of nonlinear aero elasticity [24]. In the practice of designing and production of new rotorcraft, a full-scale test of the basic prototype is needed before the first flight. This is done due to the requirement to reduce the risk of losing a high-cost item and to minimize the risk of the test operator. In such a test, the reliability of functioning of all rotorcraft systems should be checked, especially, the control system, as well as the strength of the structure at all stages of the flight. However, under the dynamic loading the type

and parameters of testing equipment can significantly affect the level and distribution of stresses and strains, as well as their changes over time. In turn, the planning and preparation of these tests requires accurate designing of the test setup, its control system, a preliminary analysis of the dynamic behaviour of the system “test setup – object”.

As a result of the review, the goal and objectives of the study were formulated.

### 3. Analytical study and computer-aided simulation of dynamic properties of aircraft component in full-scale test

#### 3.1. Properties of solutions of the structural dynamics of elastic systems

The general solution of the linear dynamic problem of an elastic system is described by a system of ordinary differential equations or partial differential equations. Each such set of equations has an infinite number of solutions among which there is a unique solution to a specific problem. It is determined by the boundary conditions. In other words, the properties of the external and internal constraints are determined by the external supporting and interaction between the parts of the dynamic system. For example, for the one-dimensional problem, the number of permanent integration coincides with the number of superimposed ties. In the practice of real system analysis, the properties of the boundary conditions are often simplified: absolutely rigid supports, perfectly smooth contact surfaces (frictionless). These are the so-called classical boundary conditions. Obviously, the real systems do not have any classical boundary conditions. In each case, the effects of possible deviations should be evaluated. If necessary, the boundary conditions can be described in more detail to provide a correct result.

This paper analyses the ways of obtaining the estimates of the effect of boundary conditions and some general regularities of this effect.

#### 3.2. Simple example. A cantilever beam with an elastic clamping

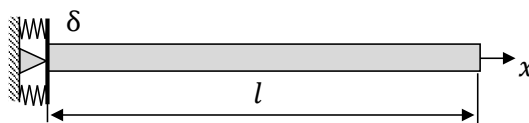


Fig. 3.1. A cantilever beam with an elastic rotational support

In this example, the analysis of the system permitting a simple analytic solution is carried out. It allows to show some general regularities of the effect of boundary conditions on the dynamic characteristics of the elastic system. The transverse free oscillations of the thin uniform beam with elastic support are analysed.

The solution of a differential equation of the beam bending allows to obtain the general solution of the beam shape  $V(x)$  of the normal vibration mode:

$$V(x) = C_1 \cosh kx + C_2 \sinh kx + C_3 \cos kx + C_4 \sin kx, \quad (3.1)$$

where  $k$  is a root of characteristic equation.

The integration constants  $C_1, C_2, C_3, C_4$  are defined by the boundary conditions. For the cantilever beam (Fig. 3.1), they can be expressed as follows:

$$V(0) = 0, \quad V'(0) = \delta DV''(0), \quad V''(l) = 0, \quad V'''(l) = 0.$$

This creates a system of four linear homogeneous algebraic equations for determining the integration constants  $C_1, C_2, C_3, C_4$ . This system has a non-trivial solution if the matrix of coefficients is equal to zero. The frequency equation in this case is:

$$\cosh kl \cos kl + \bar{\delta}kl(\cos kl \sinh kl - \sin kl \cosh kl) + 1 = 0, \quad (3.2)$$

where

- $\bar{\delta} = \frac{\delta}{l/D}$  – relative compliance of the support;
- $\delta$  – rotational compliance of the support;
- $D$  – bending stiffness of the cantilever beam cross-section.

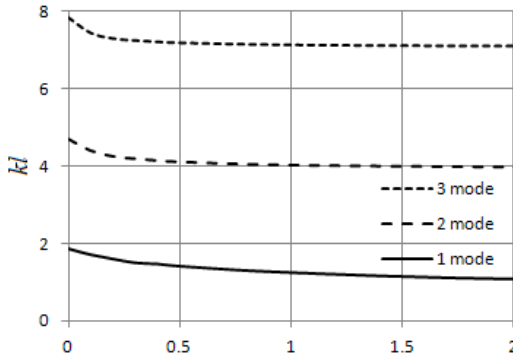


Fig. 3.2. Natural frequencies as functions of relative compliance of support

The roots  $kl$  of the frequency equation define the spectra of beam eigenfrequencies.

$$f_n = \frac{(kl)_n}{2\pi l^2} \sqrt{\frac{D}{m}}, \quad (3.3)$$

where

$m$  – mass of the beam unit length;

$n = 1, 2, \dots$  – the number of the mode of oscillations.

In Fig. 3.2, the natural frequencies as the function of elastic compliance are presented for the first three modes. A monotonic decrease of all natural frequencies is observed. If the compliance coefficient tends to infinity (disappearance of constraints), the first natural frequency tends to zero, so that the oscillatory form disappears. Higher natural frequencies have nonzero limits, and for higher mode the rate of approaching to this limit is greater. In other words, if the mode of oscillation is higher, the natural frequency of this mode and its shape is less sensitive to a change of the elastic compliance of the support.

### 3.3. Dynamic properties and response of the structure

Here a general mathematical description is presented of the complex elastic system that can be released by computational simulation for practical applications. Some elastic body or system of  $m$  bodies in the region  $W = \cup_{j=1}^m (W_j)$  bounded by the external surface  $S$  are considered. Internal

constraints are defined on the subbodies contact surfaces  $S_{ij} = S_i \cap S_j$ , and the external boundary conditions are given on the other part of surface  $S$ . The displacement vector  $\mathbf{u}(\mathbf{x}, t)$  is defined by the following motion equation:

$$\rho(\mathbf{x})\mathbf{u}(\mathbf{x}, t) = L(\mathbf{u}) + \mathbf{p}(\mathbf{x}, t), \quad (3.4)$$

where

- $L(\mathbf{u})$  – a linear operator of the displacement vector  $\mathbf{u}(\mathbf{x}, t)$ ;
- $\mathbf{p}(\mathbf{x}, t)$  – an intensity of the excitation force;
- $\mathbf{x}$  – a vector of coordinates of a point.

For example, the operator  $L(\mathbf{u})$  view of isotropic elastic body is

$$L(\mathbf{u}) = \lambda \text{grad}(\text{div } \mathbf{u}) + \mu \Delta \mathbf{u}, \quad (3.5)$$

where  $\lambda$  and  $\mu$  are Lamé constants.

Equation (3.3) can be resolved by the separated variables method as follows:

$$\mathbf{u}(\mathbf{x}, t) = U(\mathbf{x})\theta(t). \quad (3.6)$$

This solution exists if the function  $U(\mathbf{x})$  is some eigenmode of the next ordinary differential equation:

$$L(U) + \omega^2 \rho(\mathbf{x})U(\mathbf{x}) = 0. \quad (3.7)$$

The non-trivial solution  $U_k(\mathbf{x})$  (shape of the eigenmode) of Equation (3.9) exists for some spectrum of eigenvalues (natural frequencies)  $\omega_k$ , ( $k = 1, 2, \dots, \infty$ ).

At forced oscillation, the dynamic response of an elastic linear dynamic system under some external load can be described as a modal decomposition of the displacement vector  $\mathbf{u}(\mathbf{x}, t)$  to the basic system of functions  $U_k(\mathbf{x})$  ( $k = 1, \dots, \infty$ ). As a result, the vector of displacements can be presented by series

$$\mathbf{u}(\mathbf{x}, t) = \sum_{k=1}^{\infty} U_k(\mathbf{x})\theta_k(t), \quad (3.8)$$

where  $\theta_k(t)$  is a so-called normal function, which is a solution of the following ordinary differential equation:

$$M_k \ddot{\theta}_k(t) + M_k \omega_k^2 \theta_k(t) = \Phi_k(t), \quad (3.9)$$

where  $M_k = \iiint \rho(\mathbf{x})U_k^2(\mathbf{x})dV$ ,  $\Phi_k(t) = \iiint \mathbf{p}(\mathbf{x}, t)U_k(\mathbf{x})dV$  is a modal mass of the system and a modal force respectively associated with the  $k$ -th mode of free oscillations.

The dynamic response  $\mathbf{u}(\mathbf{x}, t)$  at a harmonic excitation by the force  $\mathbf{p}(\mathbf{x}, t) = \mathbf{p}_0(\mathbf{x})e^{i\omega t}$  can be expressed by the following series:

$$\mathbf{u}(\mathbf{x}, t) = e^{i\omega t} \sum_{k=1}^{\infty} \frac{U_k(\mathbf{x})\Phi_{k0}}{M_k(\omega_k^2 - \omega^2)}, \quad (3.10)$$

where  $\Phi_{k0} = \iiint \mathbf{p}_0(\mathbf{x})U_k(\mathbf{x})dV$  and  $\mathbf{p}_0(\mathbf{x})$  is an amplitude of modal force.

## **4. Vibration-based detection of structural damage in full-scale test**

### **4.1. Fundamentals of method (dynamic properties, dynamic response to different types of excitation, EMA and OMA approaches of dynamic properties evaluation and damage detection, board band excitation and frequency response function, transience function)**

Vibration-based damage detection is one of the most attractive for structural health monitoring (SHM). As modal characteristics of a structure are directly related to physical properties of the structure, (mass, stiffness, and damping), they can be used to detect, locate, and characterize damage in the structure [27]. There are large number of research and developments in mechanical, civil, and aerospace engineering dedicated to vibration-based damage detection. Some corresponding review-information can be found in [2]–[8], [28]. Methods that use changes of natural frequencies due to presence of damage usually require simple vibration measurements for estimation of position and growth of damage after calibration or accurate physics-based simulation. The mode shapes directly provide also spatial information of structural changes due to damage. Curvature mode shapes can be more sensitive and more effectively used to identify damage [29], [30].

Two basic techniques are used for practical realisation of the vibration-based damage detection. Traditional is the experimental modal analysis (EMA) that allows more completely and accurately to identify damage. However, the EMA requires the measurement of both the input and the output of dynamically loaded structure. Operational modal analysis (OMA) uses output only, is cheaper and faster than EMA and can be easily applied to large structure [14].

The Thesis has investigated the principal problems of the local system of SHM of large scale aircraft component. Vibration-based damage detection is accepted as a basic condition, and main attention is focused on a low-cost solution that would be attractive for practice.

### **4.2. General problems of vibration-based method (VBM) application**

The global aim of research is a problem of application of vibration-based method of NDT for SHM based on a solution for a relatively small structural damage detection using operational low-frequency excitation (OMA approach).

It is known that the direct modal analysis is either low sensitive or difficult for practical application in operation. If the scale of damage is small in comparison with structure dimensions, then the effect of damage is significant only for higher modes of structure. For example, there is a number of analytical and experimental investigations of crack or additional small mass effect on dynamic properties of the cantilever beam [31]–[36], which confirm appreciable shift of separate higher natural frequencies only and change of corresponding mode shapes. Later ones show location of damage, but for the reliable indication of damage the branched net of sensors is needed.

Theoretically any response of linear dynamic system is a linear combination of all modes. The principal question is: whether the effect of damage is sufficient for its detection of the available vibration-based technique of NDT. Another question is associated with the fitness of this technique for implementation in the SHM system. An acceptable solution could be found if its application is a priori restricted by some conditions. The main of them is the restriction of dimensions of the monitored zone of structure. In other words, the SHM system should be local. The second condition accepted in

this paper is that the SHM system should be objectively oriented (the type of damage, its location, acceptable detectable size should be known). At those conditions the local vibration-based SHM system can be developed and has some perspective of practical application in operation.

More detailed description of investigation aim is given further.

There is a large full-scale component of some structure. In a fixed zone of structure, a structural damage is expected. A few sensors are embedded in this zone for vibration measurement at low frequency excitation. More precisely, the excitation basic frequency is close to the first natural frequency of full structure and is much smaller than the first “local” natural frequency of a monitored zone. The investigation of this problem and development of an approach of extraction of damage features is the aim of the Thesis.

### 4.3. The basic idea of innovative approach of a damage detection by VBM: the use of group evolution of higher modes

The effect of damage on dynamic properties of a structure was estimated by general linear model of structure with embedded small 1D oscillator. Later, the local mass/stiffness variation of structure parameters due to a damage was simulated. Finally, the dynamic response of linear system at harmonic excitation could be presented in Equation (4.3.1).

$$\mathbf{u}(\mathbf{x}, t) = \sum_{k=1}^{\infty} \mathbf{U}_k(\mathbf{x})\theta_k(t), \quad (4.3.1)$$

where  $\mathbf{U}_k(\mathbf{x})$  and  $\theta_k(t)$  are the modal vector and the normal function of the  $k^{th}$  mode of free oscillation. Note that the modal vector corresponds to intact structure.

At harmonic excitation with a circular frequency  $\omega$  the normal function of the  $k^{th}$  mode is

$$\theta_k(t) = A_k(\omega)e^{j\omega t} \quad (4.3.2)$$

$$A_k(\omega) = \frac{(1 - \bar{\omega}^2)\Phi_k}{[M_k(1 - \bar{\omega}^2) + m(\boldsymbol{\xi}_0)\mathbf{u}(\boldsymbol{\xi}_0)\mathbf{U}_k(\boldsymbol{\xi}_0)](\omega_{dk}^2 - \omega^2)}, \quad (4.3.3)$$

where  $M_k$  and  $\Phi_k = \iiint \mathbf{F}_0(\boldsymbol{\xi})\mathbf{U}_k(\boldsymbol{\xi})dW$  are the modal mass and modal force of the  $k^{th}$  mode. The modal frequency of damaged structure  $\omega_{dk}^2$  is defined in Equation (4.3.4).

$$\omega_{dk}^2 = \omega_k^2 \left[ 1 + \frac{m(\boldsymbol{\xi}_0)\mathbf{u}(\boldsymbol{\xi}_0)\mathbf{U}_k(\boldsymbol{\xi}_0)}{M_k(1 - \bar{\omega}^2)} \right]^{-1}, \quad (4.3.4)$$

where  $\mathbf{u}(\boldsymbol{\xi}_0)$  is a vector-amplitude of oscillation of main structure in the base of oscillator. Excitation relative circular frequency  $\bar{\omega}$  is given in respect to the natural frequency of oscillator.

Equations (4.3.3) and (4.3.4) define the effect of damage on modal frequency and amplitude of harmonically forced vibration. From Equation (4.3.4) it can be seen that this effect can be appreciable only for the mode with modal and excitation frequencies close to the natural frequency of oscillator and at the condition that the mass of equivalent oscillator is not very small in comparison with modal mass  $M_k$ . The effect of damage is more complex and defined by variation of modal frequency and modal mass.

So, the effect of small damage practically cannot be reliably detected at low-frequency excitation in the conditions of formulated problem using only modal analysis of output signal. However, in

practice, the input signal often contains high-frequency components (for example, white noise). In this case, high eigenfrequencies due to local design properties of structure can be detected in the spectral decomposition of the output signal. It is obvious that a small-size defect most significantly affects the dynamic response of the structure in the damaged zone. For this purpose, an analysis of the local dynamic properties of the object of investigation was carried out. The tested tail beam has a thin-walled quasiperiodic structure. Its elementary structural unit is the skin fragment bounded by two adjacent stringers (in the circumferential direction) and two adjacent frames (in the longitudinal direction).

Further are presented the results of a local modal analysis of small 0.5 mm thin-walled panel of the tail beam. The cylindrical panel with a 450 mm curvature radius simulates a portion between two frames (distance 372 mm) and covers three stringers (Fig. 2, a)). The total length of a curved edge of a panel is equal to 218 mm. The pin-type boundary condition is selected at all contour of a panel. As a result, the conditions of dynamic behaviour of middle stringer and close part of a skin were estimated as similar to the same part in assembled structure. The Autodesk Inventor was used for both geometrical simulation and modal FEA.

In Fig. 4.1 the CAD model of a panel, and its views with two types of pseudo-damage (PD) are shown. A more detailed description of PD is given below.

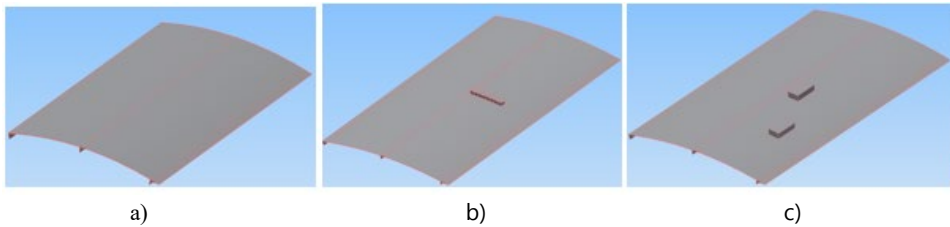


Fig. 4.1. The model of a panel for intact structure (a), for the SPD (b), and for the LPD (c).

Several results of modal FEA are presented in Fig. 4.2. The first natural frequency is equal to 367.91 Hz for intact panel, 383.08Hz for SPD, and 274.63 Hz for LPD.

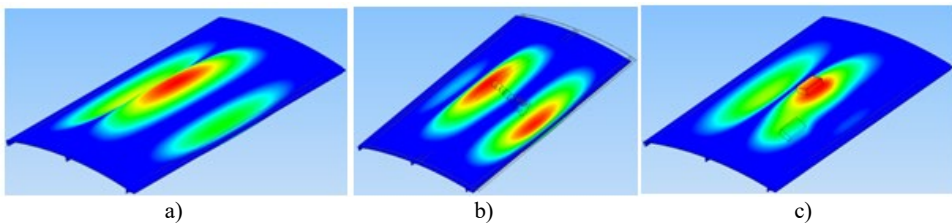


Fig. 4.2. The first mode of a panel for intact structure (a), for the SPD (b), and for the LPD (c)

So, a small damage of structure is able appreciably to affect local dynamic properties of some small part of structure. It is seen also that such damage effect on general dynamic properties of a structure is limited by the local changing of shape of the mode the natural frequency of which is closest to the local natural frequency of the damaged zone.

## 5. Experimental study and method validation

### 5.1. Full-scale calculation used in the test

#### 5.1.1. Study of the tail boom of the Mi-8 helicopter

##### Short description of the full-scale structural component of aircraft

The helicopter Mi-8 tail beam structure was selected for experimental investigation (general view in Fig. 5.1). The beam has the form of the truncated cone with a length of 5485 mm, and the diameters of end cross-sections are 1000 and 550 mm, respectively. The material of all main elements of the beam is the aluminium alloy D16AT (close to Al2024-T3). A skin thickness is in interval 0.5–0.8 mm. Stringers (total number 26) of angular cross-section are connected to the skin by spot-welding. The 17 frames are riveted to the skin. There are a number of non-regularities of structure of the beam due to technological and operational requirements (hatches, connection units, transmission supports, etc.) that are the potential sources of skin damaging in operation.



Fig. 5.1. General view of the helicopter Mi-8 tail beam (a) and the test setup for dynamic loading (b); 1– the tail beam, 2 – imitator of the tail rotor beam, 3 – the eccentric shaker.

### 5.1.2. Study of the tail boom of the Ka-62 helicopter

For the experimental investigation of the dynamic response to pulsed excitation, the tail boom structure of the Ka-62 helicopter was used.

Figure 5.2 shows the tail boom in the design of the Ka-62 helicopter (structural groups).

The general view of the beam on the test bench is shown in Fig. 5.3.

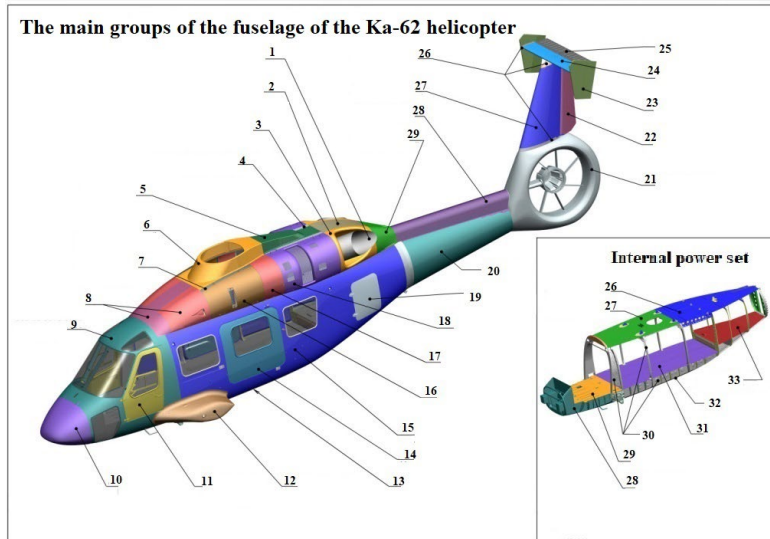


Fig. 5.2. Constructive groups of the Ka-62 helicopter.



Fig. 5.3. The tail beam of the Ka-62 helicopter on the test bench.

The beam has the shape of a truncated cone.

Geometrical parameters of the tail boom:

- length 2.70 m;
- the largest diameter 1.05 m;
- the smallest diameter 0.61 m.

The power set of the beam is a skin, spars, and stringers. The material of these elements is aluminum alloy D16. The thickness of the skin is 0.8 mm. Four spars are located at an angle of 45 degrees to the vertical line. Three stringers are located between the upper spars (Fig. 5.4 a)). A special feature of the design of the tail boom of the Ka-62 helicopter is the use of composite panels. Composite panels are installed inside between the side members in the side and the bottom (Fig. 5.4 b)). Composite panels are connected to the skin by rivets. The thickness of the plating package and composite panel is 10 mm.

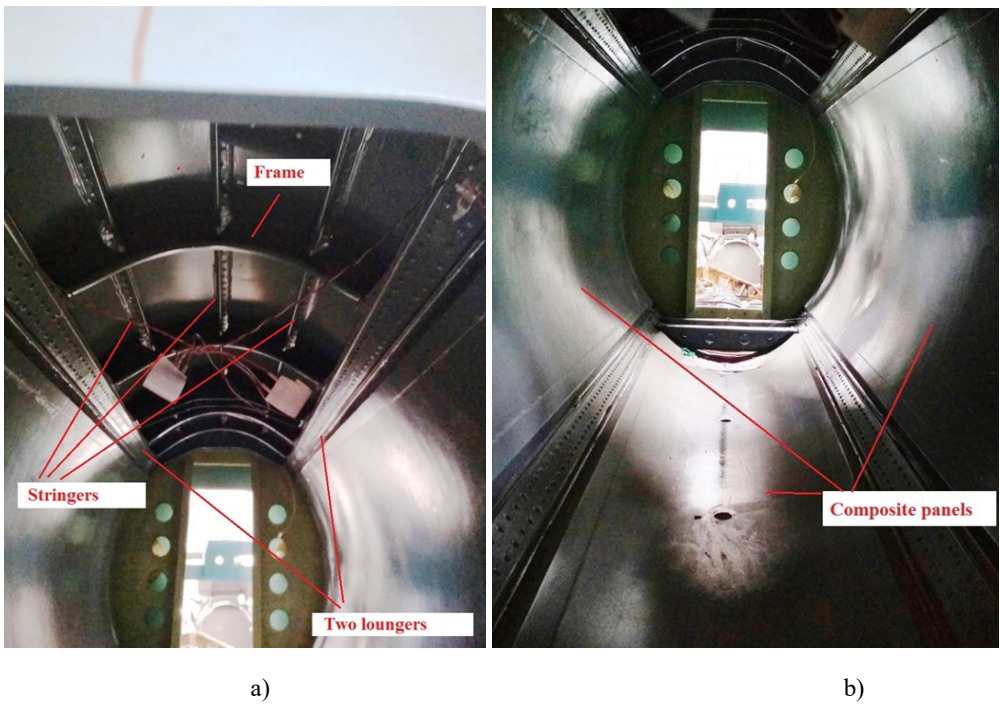
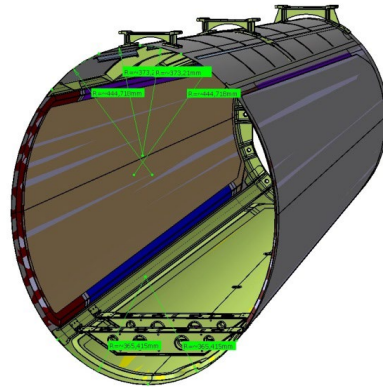


Fig. 5.4. Power beam set.

To obtain a signal from the impulse action on the tail boom, there are three strain gauges (Fig. 5.5 a)). In the figure, numbers 1, 2, and 3 show the location of the strain gauges.

Based on the geometric data, a computer model of the beam box is compiled to determine the expected frequencies at which the response can be obtained (Fig. 5.5 b)). Impulse action on the beam was in the form of a shock in the vertical plane on the flange in the end part of the beam.



a)

b)

Fig. 5.5. Location of strain gauges (a) and computer model (b).

To obtain a diagnostic test of impulse action, the method of loosening the bolted joint at the junction of the tail boom and the fuselage was used. At the stand, the fuselage was imitated by a bench plate.

Figure 5.6 shows the places of weakness of bolted connections.

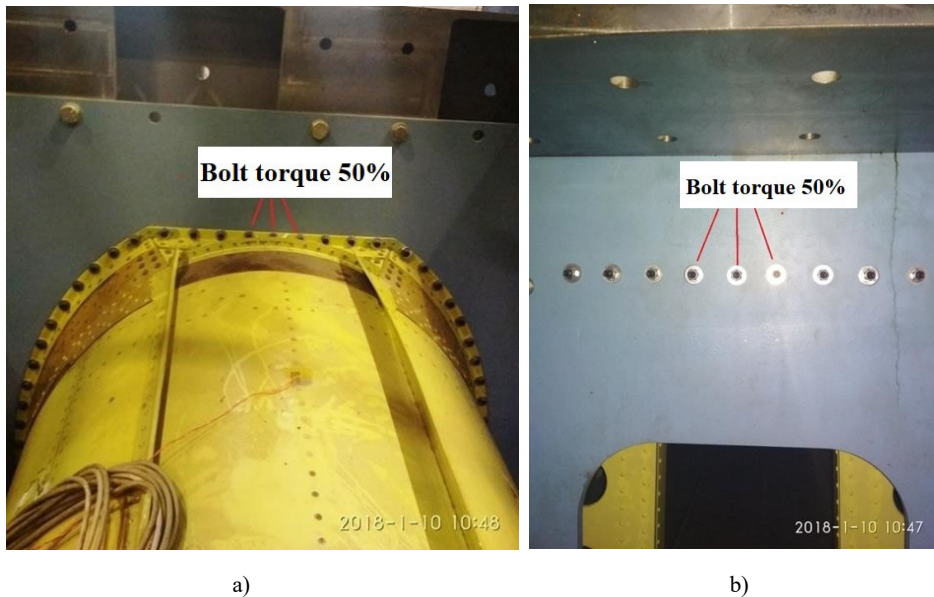


Fig. 5.6. The place of easing of the tightening of bolts in the flange connection of the tail boom and fuselage: a) view of the direction of flight; b) view versus the flight direction.

## 5.2. The objectives of the test and equipment

### 5.2.1. The objectives of test

1. Measurement of the strain/stress state of an aircraft full-scale component at dynamic loading.
2. Experimental investigation of pseudo-damage effect to the strain/stress state of skin of the tail beam at nominally harmonic excitation.

### 5.2.2. Test setup

The test setup consists of the test portal as a base for fixing of the tail beam, the imitator of the tail rotor beam, and the eccentric shaker with electromechanical drive (Fig. 5.1 b)). In contrast to usual practice of vibration test, the strain gauge technique was used for the dynamic measurement. Two strain gauge rosettes were pasted in zone 2 of the outer surface of a skin. In Fig. 5.7 a), the rosette in zone 2 is shown.

The technology of pseudo damage was used for damage effect simulation. Pseudo damage is a non-destructive modification of a test object, which affects local dynamics properties of a tested structure [19]–[21]. The small pseudo damage (SPD) was completed as a row of eight  $6 \times 6 \times 6$  mm steel blocks (total mass 12 g) and placed in zone 1 (Fig. 5.7 b)). Two steel blocks (total mass 26 g) were pasted in zone 2 and qualified as large pseudo damage (LPD).

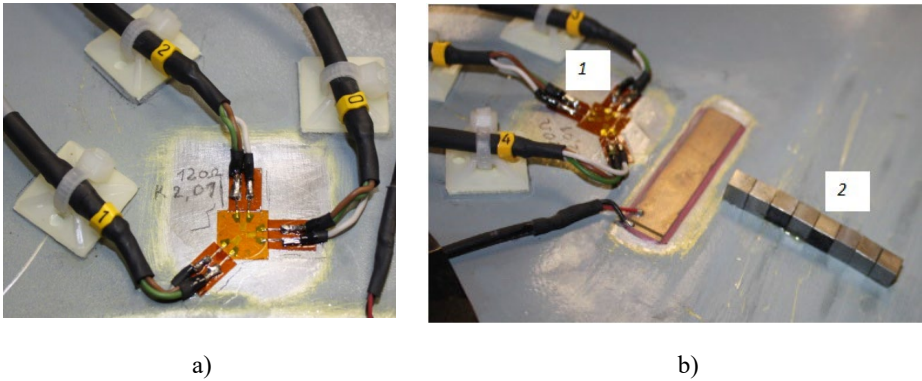


Fig. 5.7. A rosette of three strain gauges (a) and a strain gauge rosette with the small pseudo damage (SPD) in zone 2 (b).

Dynamic strain was measured by the multichannel oscilloscope NI PXIe-4330, 16Ch, 24-Bit, 25 kS/s Bridge Input Module and PC with NI LabVIEW software. The sampling rate of 5 kS/s and the length of a record – 5 s – were accepted as optimal for the data acquisition sufficient for the aim of experimental study. Cyclic excitation of vibration was limited by frequency band close to the first natural frequency of a beam (3.9 Hz).

### 5.3. Test results

The main results of the test for excitation frequency 3.8 Hz are presented below. Using strain measurement data, the components of plain stress state  $\sigma_x$ ,  $\sigma_y$ ,  $\tau_{xy}$  were defined in both zones. It is

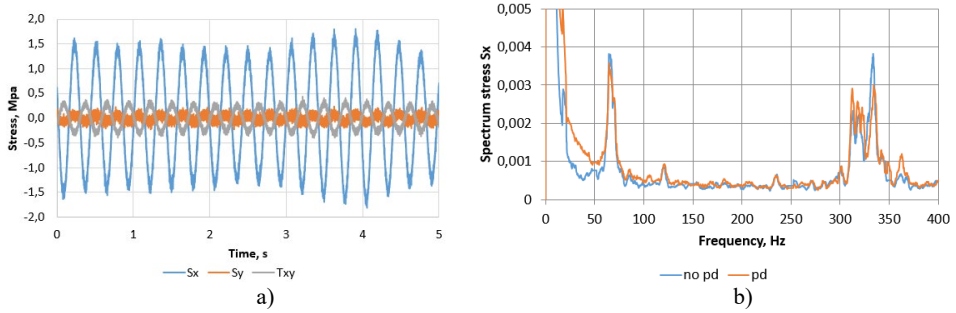


Fig. 5.8. The components of stress state in zone 1 as time functions (a) and spectrum of stress component  $\sigma_x$  in the frequency band 0-400 Hz in zone 1 (b).

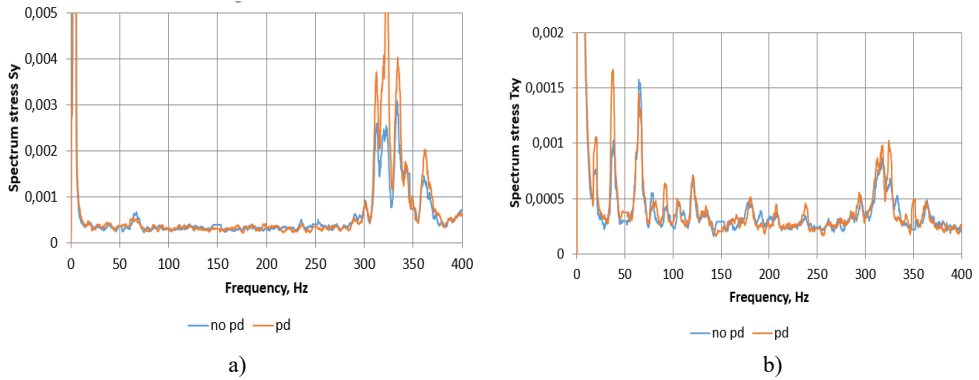


Fig. 5.9. Spectrum of stress component  $\sigma_y$  (a) and stress component  $\tau_{xy}$  in the frequency band 0-400 Hz in zone 1.

accepted that the axis  $x$  coincident with longitudinal direction of a beam and the axis  $y$  is perpendicular to first one.

Typical stress/time functions are shown in Fig. 5.8 a) for stress state in zone 1. Fast Fourier transform (FFT) was done for each of three stress components (Figs. 5.8 b) and 5.9) for intact and structure with a pseudo-damage. Similar results for zone 2 with LPD are presented in Fig. 5.10. Spectral transform allows to define directly the resonance frequencies 3.9, 20.6 Hz, 38.6 Hz, and 65.0 Hz, which was confirmed also by the direct measurement in the process of dynamic test. Significant peaks of spectrum are also at frequencies 83.8 Hz, 121.2 Hz, and 136.6 Hz. It can be seen that any shift of the mentioned resonance frequencies is not observed at the presence of PD. In the

frequency band 150–275 Hz the amplitude of spectrum is distributed with a relatively small fluctuation. The amplitude of spectrum sharply increases in the frequency band 275–400 Hz.

The spectrum of all components of stress for structure with PD is close to corresponding spectrum of the intact structure.

An interesting result is obtained for the spectrum of stress component  $\sigma_y$  (lateral direction): the amplitude of spectrum is large practically in the frequency band 275–400 Hz only (Fig. 5.10).

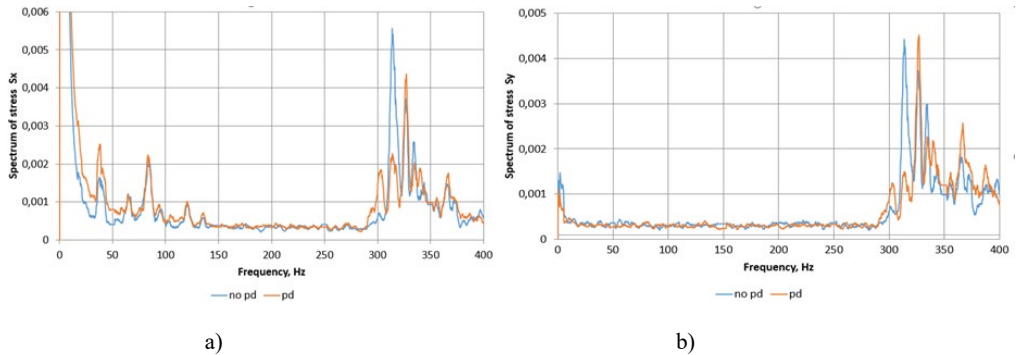


Fig. 5.10. Spectrum of stress component  $\sigma_x$  (a) and stress component  $\sigma_y$  (b) in the frequency band 0–400 Hz in zone 2

#### 5.4. Discussion and feature extraction

As noted above, the tested beam has a quasiperiodic structure. Therefore, it can be assumed that there is an interaction of neighbouring structural units and the existence of many eigenmodes of the beam vibration in a narrow frequency band. Indeed, an additional modal analysis of the more complex part of the beam that consists of 39 structural units shows that there are at least fifteen independent eigenmodes in the frequency band 280–390 Hz. In the same limits, intensive increasing of response spectrum is observed in the test (Figs. 5.8–5.10). This can be explained by the presence of a close spectrum of natural frequencies in the band 275–400 Hz.

At the same time, changes in the spectral power of response due to the appearance of damage can be seen. Moreover, the complexity of the dynamic response spectrum in the frequency band of interest causes difficulties of defect identification by the shift of the natural frequency and the change in the shape of the modes.

Therefore, variants of the integral estimation of the change in the response spectrum were considered. The most successful is the use of the correlation coefficient deviation (CCD) index that is widely used in different applications [22]–[25].

$$CCD = 1 - CC, \quad (5.1)$$

where

$$CC = \frac{cov(x,y)}{s_x s_y}, \quad (5.2)$$

$cov(x, y)$  is the covariance between two sample random vectors  $x$  and  $y$ , which are the spectrum of response of intact and damaged structures, respectively, in the selected frequency band, and  $s_x, s_y$  are the standard deviations of random vectors. It is seen that the  $CCD$  index is equal to zero, if there is not any damage effect, and cannot be more than 1. The larger value of the  $CCD$  index corresponds to higher effect of damage.

In Fig. 5.11, the comparison of  $CCD$  indices of damaged (with LPD and SPD) structures are shown for the spectrum of dynamic response at excitation nominal frequency 3.8 Hz. It is seen that the  $CCD$  index increment due to pseudo-damage is observed for all stress components. At the same time, the damage effect is greater for a larger pseudo-defect.

The important aspect of this index application is the requirements to input signal. A general assumption in the theory of OMA concerns the input, which is not measured and consists of a Gaussian white noise with a flat spectrum in the frequency band of interest [12]. At the nominally harmonic excitation with frequency close to

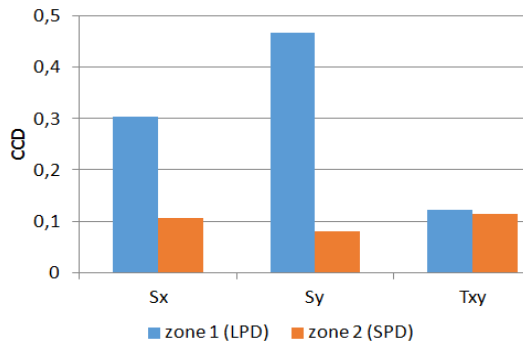


Fig. 5.11. Effect of pseudo-damage on CCD index.

first resonance the intensities of output for intact and damaged structures may be different. Therefore, the processing of each record of the output signal must provide its normalization before the operation of determining the index. The mean amplitude of output was used here as acceptable estimate of output intensity.

## 6. Statistical estimation of perspective damage index for vibration-based structural health monitoring

### 6.1. Test setup and measuring equipment

The helicopter Mi-8 tail beam structure was selected for experimental investigation (Subsection 5.2.2).

The strain gauge technique was used for the dynamic measurement. Two strain gauge rosettes were pasted in two zones of the outer surface of a skin (Fig. 5.7). Dynamic strain was measured by the multichannel oscilloscope NI PXIe-4330, 16Ch, 24-Bit, 25 kS/s Bridge Input Module and PC with NI LabVIEW software. The sampling rate 5 kS/s and the length of a record of 5s were accepted as optimal for the data acquisition enough for the aim of experimental study.

The forced vibration of the beam was excited by the mechanical eccentric shaker with control of excitation frequency. In the analysis presented below there are used the dynamic responses of a beam at the cyclic excitation with basic frequency 3.55 Hz (close to the first natural frequency of a beam) and low amplitude vibration in the frequency band of interest (white noise).

The technology of pseudo damage was used for damage effect simulation. The small pseudo damage (SPD) was completed as a row of eight  $6 \times 6 \times 6$  mm steel blocks (total mass 12 g) and placed in zone 2 (Fig. 5.7 b)). Two steel blocks (total mass 26 g) were pasted in zone 2 and qualified as the large pseudo damage (LPD).

### 6.2. Important results of the research

The dynamic response in frequency domain was obtained for each stress component (two examples for  $\sigma_x$  and  $\sigma_y$  in Fig. 6.1) for intact (solid) and structure with a pseudo-damage (dash). It can be seen that in the frequency band 275–400 Hz multiple resonances are observed.

The spectrum stress component  $\sigma_y$  is especially interesting. In the relatively low frequency band, the frequency response is very weak. And in the above-mentioned frequency band there is a sharp increase in the spectrum. Moreover, for all components of the stress tensor, the response to the appearance of pseudo-damage is clearly observed.

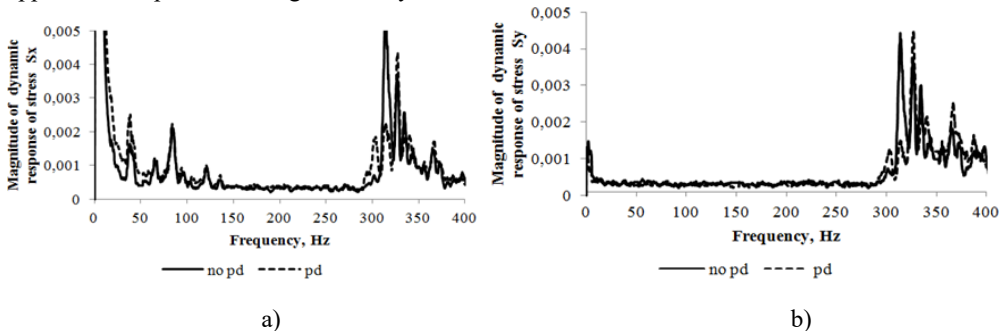


Fig. 6.1. The dynamic response of stress component  $\sigma_x$  (a) and  $\sigma_y$  (b) in the frequency band 0–400 Hz in zone 1.

### 6.3. Data acquisition and statistical analysis

To obtain the test data for the statistical analysis, 10 series of measuring of dynamic strains at the checkpoints of the intact structure and in the presence of pseudo-damage were carried out. Time record length was chosen to be 1 second at a sampling frequency of 5000 points. Pre-processing of each record includes signal centering and filtering in the frequency band 250–400 Hz. The band pass filter was designed by IIR method (Butterworth). Fast Fourier transform (FFT) and light smoothing (with span 7) of frequency response function was done at the final step of pre-processing. As a result, ten samples of the dynamic frequency response were obtained for each of six strain gauges. An example of this type of outcome for the longitudinal strain gauge of zone 1 is presented in Fig. 6.2.

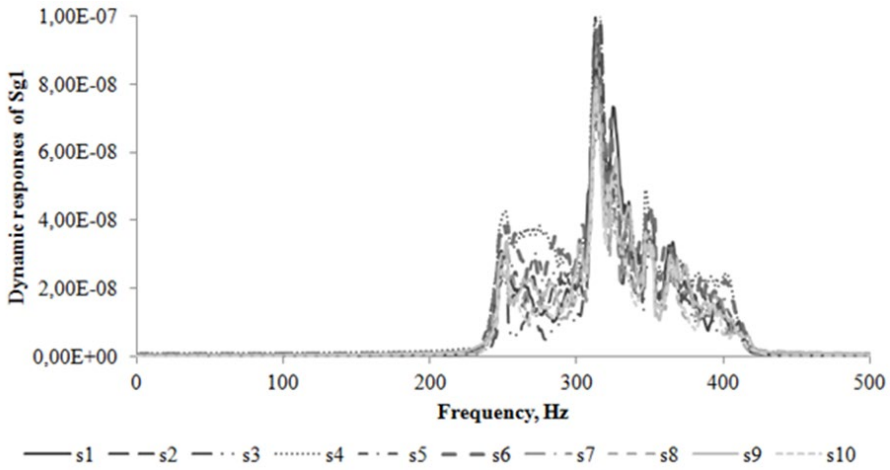


Fig. 6.2. Frequency response of the strain gauge sg1 after filtering and FFT (intact structure)

The data set for final statistical analysis contains two sets for each of the strain gauges. The set size is ten observations, each of which represents the frequency response in the band 250–400 Hz and has a size of 500 points.

The matrix  $A_k(500,10)$  contains ten observations of the intact structure frequency response measured by the strain gauge  $k$ , and the matrix  $B_k(500,10)$  is the same for pseudo-damaged structure.

The final statistical analysis consists of three steps.

Step 1: Analysis of the inter-sensor correlation in a separate loading session. In such case, the dynamic response of all strain gauges is caused by the same external load. This means that in a linear system, the strain components must be strictly proportional to each other and the correlation coefficient between them must be 1. Deviation from 1 may be caused by the influence of the measurement accuracy and/or nonlinearities of a structure.

The correlation coefficient  $C_{km}^{(n)} = \text{corrcoef}(A_k(:,n), A_m(:,n))$  between random variable  $A_k(:,n)$  and  $A_m(:,n)$  of observation (test option)  $n$  was calculated for intact structure, and similarly,

for pseudo-damaged structure  $C_{km}^{(n)} = \text{corrcoef}(B_k(:, n), B_m(:, n))$ . For strain gauges of zone 1  $k = 1$  and  $m = 2, 3$ , and for zone 2  $k = 4$  and  $m = 5, 6$ ,  $n = 1, 2, \dots, 10$ .

Outcome of this analysis is presented in Table 6.1.

Table 6.1

The mean and minimum values of the correlation coefficient

State of structure	Value of parameter	$C_{12}$	$C_{13}$	$C_{45}$	$C_{46}$
Intact	Mean	0.99995	0.99995	0.99999	0.99999
	Minimum	0.99984	0.99984	0.99991	0.99991
Pseudo-damage	Mean	0.99997	0.99996	0.99991	0.99990
	Minimum	0.99989	0.99990	0.99975	0.99972

The mean value of correlation coefficient for all data set is equal to 0.99997, and the minimum is 0.99987. It means that the inter-sensor correlation in a separate loading session is very close, the accuracy of the measurements is relatively high, and the effect of nonlinearities is insignificant.

Step 2: Estimation of load scattering effect on the dynamic response of a separate strain gauges and the distribution law of CCD. The mean vectors of all observations for each strain gauge were obtained for both intact and pseudo-damaged state of a structure.

$$\bar{A}_k = \sum_{n=1}^{10} A_k(:, n) \quad \bar{B}_k = \sum_{n=1}^{10} B_k(:, n) \quad (6.1)$$

The correlation coefficients are:

$$C_{k0}^{(n)} = \text{corrcoef}(A_k(:, n), \bar{A}_k) ; \quad C_{k1}^{(n)} = \text{corrcoef}(B_k(:, n), \bar{B}_k), \quad (6.2)$$

and the correlation coefficient deviation (CCD)

$$CCD_{k0}^{(n)} = 1 - C_{k0}^{(n)} \quad CCD_{k1}^{(n)} = 1 - C_{k1}^{(n)} \quad (6.3)$$

can be introduced as the signatures of deviation of any observation from averaged value due to the specific load at given state of a structure. The mean values of the CCD for all six strain gauges are presented in Table 6.2.

Table 6.2

The mean values of the correlation coefficient deviation of dynamic response

State of structure	sg1	sg2	sg3	sg4	sg5	sg6
Intact	0.04147	0.03588	0.06115	0.10023	0.04093	0.05373
Pseudo-damaged	0.21180	0.10863	0.06877	0.13966	0.04489	0.05579

Thus, estimates of the effect of load variation on CCD index were obtained for two states of the system. At the same time, the installation of pseudo-damages led to an increase of CCD for two sensors in the LPD zone, which indicates the effect of a configuration change on the dispersion of CCD due to the variation in load.

The null hypothesis that the data in vector-column in  $CCD_0$  and  $CCD_1$  matrices is from a population with a normal distribution in seven tests from twelve were rejected by the Anderson–Darling test. Thus, there is not reliable evidence about normal distribution of considered random variables.

Step 3: Feature extraction. The damage index CCD corresponding to the strain gauge  $k$  frequency response in the observation  $n$  is defined by Equation (6.4)

$$CCD_k^{(n)} = 1 - C_k^{(n)} \quad (6.4)$$

The correlation coefficient  $C_k^{(n)}$  between the dynamic response of the pseudo-damaged structure in the frequency band of interest  $B_k(\cdot, n)$  measured by the strain gauge  $k$  in the observation (test option)  $n$ , and the average response  $\bar{A}_k$  of this strain gauge in the intact structure.

First of all, a test decision for the null hypothesis that the random vectors  $B_k(\cdot, n)$  and  $\bar{A}_k$  are from the same continuous distribution was done using the two-sample Kolmogorov–Smirnov test. The data set of this test decision for pseudo-damaged structure defined by Equation (5) are represented in the Table 6.3.

For five tests (sg1, sg2, sg3 – zone 1 of LPD and sg5, sg6 – zone 2 of SPD) the null hypothesis was rejected at the 5 % significance level. Only for one test (sg4 – zone 2 of SPD) null hypothesis was not rejected. This means that the CCB index uniquely detects the appearance of an LPD. The effect of the SPD on CCD is significantly weaker, which bears witness to the effectiveness of the proposed index.

Table 6.3

Data set for CCD random variables of the strain gauges

Test number	sg1	sg2	sg3	sg4	sg5	sg6
1	0.7010	0.3969	0.3682	0.1957	0.0928	0.1214
2	0.4260	0.2185	0.4995	0.1307	0.0549	0.2303
3	0.2003	0.2029	0.4052	0.0886	0.0580	0.1033
4	0.3606	0.1160	0.4448	0.1663	0.0475	0.0664
5	0.5063	0.2449	0.3808	0.2812	0.1146	0.2016
6	0.3484	0.3547	0.3445	0.2120	0.0795	0.1439
7	0.3124	0.1567	0.4091	0.0979	0.0592	0.1317
8	0.6805	0.3026	0.3668	0.3237	0.1437	0.1437
9	0.6496	0.8709	0.4902	0.1227	0.0410	0.1022
10	0.3208	0.1594	0.3042	0.1674	0.1243	0.2415
Mean	0.4506	0.3023	0.4013	0.1786	0.0815	0.1486

Comparison of the mean value of CCD indices of intact and pseudo-damaged structures is represented in Fig. 6.3. This index of intact structure is associated mainly with the variation of the external load in different test options, but the index of pseudo-damaged structure is mainly caused by a pseudo-damage effect. It is seen that for all three strain gauges (sg1, sg2, and sg3) located in zone 1 the significant increment of CCD index is observed due to presence of the large pseudo-damage. The small pseudo-damage in zone 2 also induces increasing of CCD index of all three strain gauges (sg4, sg5, and sg6), but effect of SPD is much less.

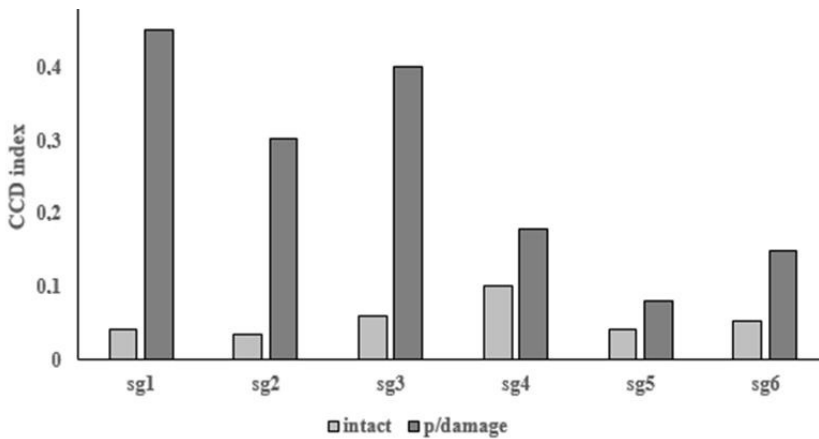


Fig. 6.3. The mean value of CCD indices of intact and pseudo-damaged structure.

## 7. Final discussion on integral damage index and conclusions

1. The importance of an adequate description of the boundary conditions for the correct result is shown. Some basic regularities of the influence of boundary conditions on the dynamic properties of an elastic dynamical system are shown. A simple example shows the specific effect of elastic matching of constraints. The increase in elastic bonds reduces the natural frequencies. It can be seen that there is some critical compatibility of support for higher modes. If the match exceeds its critical value, the corresponding mode is almost insensitive to the compliance of this restriction. A critical match for a higher regime is less. In the case of the disappearance of certain restrictions, the lower vibrational modes also disappear and their number is equal to the number of new degrees of freedom. These properties are common for an elastic system of any complexity.
2. A simplified model of an elastic beam is considered to evaluate the effect of the correspondence of boundary conditions on the main dynamic characteristics.
3. A more complex simulation of the elastic attachment of the body was made using the example of tail boom compartments of Mi-8 and Ka-62 helicopters.
4. The general problems of using the vibration non-destructive testing method for monitoring the state of a structure (SHM) in a full-scale testing of aircraft components are considered. It is shown that the solution can be found if the application of the method is limited to certain conditions. The main limitation is the limitation of the size of the controlled area of the structure, therefore, the SHM system must be local. The second condition shown in this paper is that the SHM system should be objectively oriented. This means that the type of damage, its location, and the size must be determined, must be known.  
It is shown that with certain limitations a local monitoring system (SHM) based on vibration can be developed and can be used in practice.
5. Within the framework of the operational modal analysis (OMA) approach, a solution has been developed to detect a small structural damage. In this case, the excitation of the main structure occurs at a relatively low frequency. This frequency is close to the first natural frequency of the entire structure and is much smaller than the first "local" natural frequency of the observed band.
6. An approach for the development of a prospective damage index (diagnostic feature) for detecting small lesions in a large structural component is formulated. In this case, one or more sensors should be placed in a controlled area for measuring the signal. The base level of the dynamic response of an intact structure in the accepted excitation mode determines an intact controlled structure. Comparison of the current measurement of the output signal with the baseline gives an index for evaluating the state of the structure.
7. Statistical analysis of CCD (correlation coefficient deviation) index for the structural damage detection by vibration-based method was performed. Statistic data set was collected in a full-scale

test of a large aircraft component. After special pre-processing the most informative narrow frequency band was selected for obtaining the statistic set of CCD between the frequency response functions of intact and pseudo-damaged states of a structure. The two-sample Kolmogorov–Smirnov hypothesis test was used for estimation of a pseudo-damage effect. The stable response of CCD index to a small damage in large-size structure was demonstrated.

8. The results of the research show that the problem of detecting small lesions in a large-scale structure with low-frequency excitation with an accuracy of admissible in operation can be successfully solved.

## References

- [1] J. L. Crassidis and John L. Junkins, *Optimal Estimation of Dynamic Systems. Applied Mathematics and Nonlinear Science Series*. Chapman and Hall/CRC, Boca Raton, FL, 2004.
- [2] J. P. Conte, X. He, B. Moaveni, S. F. Masri, J. P. Caffrey, M. Wahbeh, F. Tasbihgoo, D. H. Whang, and A. Elgamal, "Dynamic Testing of Alfred Zampa Memorial Bridge," *Journal of Structural Engineering, ASCE*, vol. 134, issue 6, pp. 871–1066, 2008. [https://doi.org/10.1061/\(asce\)0733-9445\(2008\)134:6\(1006\)](https://doi.org/10.1061/(asce)0733-9445(2008)134:6(1006))
- [3] B. Peeters, J. Maeck, and G. De Roeck, "Vibration-based damage detection in civil engineering: excitation sources and temperature effects," *Smart materials and Structures*, vol. 10, pp. 518–527, 2001. <https://doi.org/10.1088/0964-1726/10/3/314>
- [4] P. J. Schubel, R. J. Crossley, E. K. G. Boateng, and J. R. Hutchinson, "Review of structural health and cure monitoring techniques for large wind turbine blades," *Renewable Energy*, vol. 51, pp. 113–123, 2013. <https://doi.org/10.1016/j.renene.2012.08.072>
- [5] K. He and W. D. Zhu, "Detecting Loosening of Bolted Connections in a Pipeline Using Changes in Natural Frequencies," *ASME J. Vib. Acoust.*, vol. 136, issue 3, pp. 034503, 2014. <https://doi.org/10.1115/1.4026973>
- [6] H. Sohn, C. Farrar, N. Hunter, and K. Worden, "A Review of Structural Health Monitoring Literature: 1996–2001," Los Alamos National Laboratory report, (LA-13976-MS), 2003.
- [7] E. P. Carden and P. Fanning, "Vibration based condition monitoring: A review," *Structural Health Monitoring*, vol. 3, pp. 355–377, 2004. <https://doi.org/10.1177/1475921704047500>
- [8] C. R. Farrar, S. W. Doebling, and D. A. Nix, "Vibration-based structural damage identification," *Philosophical Transactions of the Royal Society A: Mathematical, Physical and Engineering Sciences*, vol. 359, issue 1778, pp. 131–149, 2001.
- [9] M. N. Rezai, J. E. Bernard, and J. M. Starkey, "Empirical modal analysis," *The Shock and Vibration Digest*, vol. 15, 1983.
- [10] D. J. Ewins, *Modal Testing: Theory, Practice and Application*. Baldock: Research Studies Press, UK, 2003.
- [11] M. W. Halling, I. Muhammad, and K. C. Womack, "Dynamic testing for condition assessment of bridge bents," *Journal of Structural Engineering, ASCE*, vol. 127, issue 2, pp. 161–167, 2001. [https://doi.org/10.1061/\(ASCE\)0733-9445\(2001\)127:2\(161\)](https://doi.org/10.1061/(ASCE)0733-9445(2001)127:2(161))
- [12] J. M. W. Brownjohn, P. Moyo, P. Omenzetter, and Y. Lu, "Assessment of highway bridge upgrading by dynamic testing and finite- element model updating," *Journal of Bridge Engineering, ASCE*, vol. 8, issue 3, pp. 162–172, 2003. [https://doi.org/10.1061/\(ASCE\)1084-0702\(2003\)8:3\(162\)](https://doi.org/10.1061/(ASCE)1084-0702(2003)8:3(162))
- [13] M. M. Abdel Wahab and G. De Roeck, "Dynamic testing of prestressed concrete bridges and numerical verification," *Journal of Bridge Engineering, ASCE*, vol. 3, issue 4, pp. 159–169, 1998. [https://doi.org/10.1061/\(ASCE\)1084-0702\(1998\)3:4\(159\)](https://doi.org/10.1061/(ASCE)1084-0702(1998)3:4(159))
- [14] E. Reynders, "System identification methods for (operational) modal analysis: review and comparison," *Archives of Computational Methods in Engineering*, vol. 19, pp. 51–124, 2012. <https://doi.org/10.1007/s11831-012-9069-x>
- [15] D. E. Adams, *Health Monitoring of Structural Materials and Components: Methods with Application*. Chichester: John Wiley & Sons Ltd., 2007. <https://doi.org/10.1002/9780470511589>
- [16] V. Giurgiutiu, *Structural Health Monitoring with Piezoelectric Wafer Active Sensors*. Amsterdam & Boston: Elsevier Academic Press, 2008.
- [17] G. C. Goodwin and R. L. Payne, *Dynamic System Identification: Experiment Design and Data Analysis*. Academic Press, 1977

- [18] S. A. Billings, *Nonlinear System Identification: NARMAX Methods in the Time, Frequency, and Spatio-Temporal Domains*. Wiley, 2013. <https://doi.org/10.1002/9781118535561>
- [19] T. P. Gialamas, D. A. Manolas, and D. T. Tsahalis, "Predicting the Dynamic Behaviour of a Coupled Structure Using Frequency-Response Functions," *Journal of Aircraft*, vol. 39, issue 1, pp. 109–113, 2002. <https://doi.org/10.2514/2.2902>
- [20] P. Van Loon, *Modal Parameters of Mechanical Structures*, Ph.D. Dissertation, Dept. of Mechanical Engineering, Katholieke Universiteit Leuven, Leuven, Belgium, 1974.
- [21] G. W. Housner, L. A. Bergman, T. K. Caughey, A. G. Chassiakos, R. O. Claus, S. F. Masri, R. E. Skelton, T. T. Soong, B. F. Spencer, J. T. P. Yao, "Structural control: past, present, and future," *Journal of Engineering Mechanics*, vol. 123, pp. 897–971, 1997. [https://doi.org/10.1061/\(ASCE\)0733-9399\(1997\)123:9\(897\)](https://doi.org/10.1061/(ASCE)0733-9399(1997)123:9(897))
- [22] J. T. Xing, Y. P. Xiong, and W. G. Price, "A generalized mathematical model and analysis for integrated multi-channel vibration structure–control interaction systems," *Journal of Sound and Vibration*, vol. 320, pp. 584–616, 2009. <https://doi.org/10.1016/j.jsv.2008.08.009>
- [23] G. Dimitriadis, "Bifurcation Analysis of Aircraft with Structural Nonlinearity and Free play Using Numerical Continuation," *Journal of Aircraft*, vol. 45, issue 3, pp. 893–905, 2008. <https://doi.org/10.2514/1.28759>
- [24] Hua-Peng Chen, "Nonlinear Perturbation Theory for Structural Dynamic Systems," *AIAA Journal*, vol. 43, issue 11, pp. 2412–2421, 2005. <https://doi.org/10.2514/1.15207>
- [25] Y. G. Panovko and I. I. Gubanov, *Stability and Oscillations of Elastic Systems: Paradoxes, Fallacies, and New Concepts*. Translated by Chas. V. Larrick, New York: Consultants Bureau, 1965.
- [26] S. Kuzņecovs, Ē. Ozoliņš, I. Ozoliņš, I. Pavelko, and V. Pavelko, "Dynamic Properties and Fatigue Failure of Aircraft Component," in *Engineering against Fracture: Proceedings of the 1st Conference*, Greece, Patras, 28–30 May, 2008. Amsterdam: Springer Science, 2009, pp. 105–114. ISBN 9781402094019. e-ISBN 9781402094026. [https://doi.org/10.1007/978-1-4020-9402-6\\_9](https://doi.org/10.1007/978-1-4020-9402-6_9)
- [27] S. W. Doebling, C. R. Farrar and M. B. Prime. 1998. *Shock Vib, Dig*, **30(2)** 91.
- [28] Jun Lia, and Hong Hao 2016 *Structural Monitoring and Maintenance* **3(1)** 33.
- [29] A. K. Pandey, M. Biswas and M. M. Samman. 1991. *J. Sound, Vib*, **145(2)** 321.
- [30] C. P. Ratcliffe. 2000. *ASME J Vib Acoust* **122(3)** 324.
- [31] V. Pavelko and G. Shakhmansky. 1971. *Trans. of Riga Institute of Civil Aviation* **191** 18.
- [32] I. Pavelko and V. Pavelko. 1997. *Proc. Int. Conf. (Pranesimus medziaga Transporto priemones – 97) Kaunas, Lithuania. Technology* 237.
- [33] A. Ebrahimi, M. Behzad and A. Meghdari. 2010. *Int. J. Mechl. Sci.* **52** 904.
- [34] Swapnil Dokhe, and Shailesh Pimpale, 2015. *Int. J. Res. Aer. Mech. Eng.* **3(8)** 24.
- [35] R. Y. Liang, J. L. Hu and F. Choy. 1992. *J. Eng. Mech-ASCE*. **118** 384.
- [36] D. G. Kasper, D. C. Swanson and K. M. Reichard. 2008. *Journal of Sound and Vibration* **312** 1.
- [37] H. Pfeiffer, I. Pitropakis and M. Wevers. 2010. *Proc. 10th European Conference on Non-Destructive Testing*. Moscow, www.ndt.net.
- [38] Prakash Rajendrana, and Sivakumar M. Srinivasan, 2015, *Structural Engineering and Mechanics* **54(4)** 711.
- [39] I. Pitropakis, H. Pfeiffer and M. Wevers. 2012. *Sensors and Actuators A Physical*, **176** 57.
- [40] L. W. Mays and Y. K. Tung. 1992. *Engineering and Management* McGraw-Hill, NY, USA.
- [41] A. S. K. Naidu, S. Bhalla and C. K. Soh. 2002. *Proc. SPIE*, **4935** 473.
- [42] V. Giurgiutiu, A. Zagrai and J. J. Bao. 2002. *Int. J. Structural Health Monitoring*, **1** 41.
- [43] V. G. M. Annamdas and Ch. K. Soh. 2010. *J. Intel. Mat. Syst. Struct.* **21**, 41.

- [44] А. И. Макаревский, В. М. Чижов. Основы прочности и аэроупругости летательных аппаратов. Москва: Машиностроение, 1982. –238 с.
- [45] Airworthiness of Aircraft. Annex 8 to the Convention on International Civil AviationA.
- [46] Airworthiness Manual: Volume I. Organization and Procedures by International Civil Aviation Organizatio (Creator), 412 p. Published January 1, 2001 by International Civil Aviation Organization.
- [47] Filippo de Florio. Airworthiness: An Introduction to Aircraft Certification, Elsevier, First edition, 2006, 247 p.
- [48] Airbus A380 Wing-Fuselage Testing. <https://www.youtube.com/watch?v=z19m9LZOOZY>
- [49] A-380. The wings on this Airbus flex way more than they should. [https://www.youtube.com/watch?v=-LTYRTKV\\_A](https://www.youtube.com/watch?v=-LTYRTKV_A)
- [50] Boeing 787 Wing Testing. <https://www.youtube.com/watch?v=meEG7VwjTew>
- [51] Pushing the A350 XWB to the brink. [https://www.youtube.com/watch?v=B74\\_w3Ar9nI](https://www.youtube.com/watch?v=B74_w3Ar9nI)
- [52] Boeing 787 conducts fatigue testing. <https://www.youtube.com/watch?v=TH9k9fWaFrs>
- [53] Original Wing test JS1 Revelation. <https://www.youtube.com/watch?v=M6VBqsrD4FE>
- [54] K. Irbitis. Of Struggle and Flight/ The History of Latvian Aviation, Riga, RTU Press, 2006.- (117) 211 p.
- [55] Riga, SIA “Aviatest LTD”, “Bench for testing the Ka-62 helicopter for static strength”, 2016, (17) 44 p.
- [56] "Full-size stand of the Mi-26 helicopter".
- [57] “Stand for fatigue testing of the Mi-38 helicopter fuselage” 2015, Riga, SIA “Aviatest LTD”
- [58] “Bench for fatigue testing of the fenestron of the Ka-62 helicopter” Riga, SIA “Aviatest LTD”, 97 p.
- [59] Riga, SIA “Aviatest LTD”, 2017, “Sample testing”.
- [60] Riga, SIA “Aviatest LTD”, Техническая справка № АТ-П.01-15/16г, 2016, 12 p.
- [61] Riga, SIA “Aviatest LTD”, 2014, “Elevator destruction”.
- [62] “On the Dynamic Response Prediction at the Full-Scale Test of Aircraft Component”, Transport and Aerospace Engineering, 2017, Vitaly Pavelko, Alexander Nevsky <https://tae-journals.rtu.lv/article/view/tae-2017-0003>
- [63] “Vibration-Based Detection of Small Damage in the Aircraft Large Component”, Матеріали XIII міжнародної науково-технічної конференції “ABIA-2017”, 2017, Vitaly Pavelko, Sergei Kuznetsov , Alexander Nevsky , Mark Marinbach <http://avia.nau.edu.ua/indexallua.php>
- [64] V. Pavelko , S. Kuznetsov, A. Nevsky , M. Marinbach “Vibration-Based Structural Health Monitoring of the Aircraft Large Component”, IOP Conference Series: Materials Science and Engineering, 2017, <https://iopscience.iop.org/article/10.1088/1757-899X/251/1/012093>
- [65] V. Pavelko , A. Nevsky. “Statistical Estimation of Perspective Damage Index for Vibration-Based Structural Health Monitoring”, Journal of Physics: Conference Series, 2019, <https://iopscience.iop.org/article/10.1088/1742-6596/1172/1/012036>
- [66] “Full-size stand of the Ka-62 helicopter”, 2019, SIA “Aviatest LTD”.
- [67] “Bench for testing the fatigue strength of the tail boom of the helicopter Ka-62”, 2018, SIA “Aviatest LTD”.
- [68] Health and Usage Monitoring System (HUMS) <https://www.skybrary.aero/articles/health-and-usage-monitoring-system-hums>



**Aleksandrs Ņevskis** was born in 1959 in Vitebsk, Belarus. He graduated from Riga Civil Aviation University in 1983. In 1983–1993, he was a researcher of the State Research Institute of Civil Aviation Riga branch. From 1993 to 2011, he was the Director of Rinal Plus Ltd. and from 2011 to 2022, a project manager in Aviatest Ltd.

His research interests are in the areas of dynamic and strength analysis of airframe constructions, dynamical characteristics prognostication during the airframe construction testing, and mathematical simulation.